High-resolution photoacoustic imaging with focused laser and ultrasonic beams

Fanting Kong,[1] Y. C. Chen,[1,a)] Harriet O. Lloyd,[2] Ronald H. Silverman,[2,3] Hyung Ham Kim,[4] Jonathan M. Cannata,[4] and K. Kirk Shung[4]
[1]*Department of Physics and Astronomy, Hunter College and Graduate Center, The City University of New York, 695 Park Avenue, New York, New York 10065, USA*
[2]*Weill Cornell Medical College, 1300 York Avenue, New York, New York 10065, USA*
[3]*Riverside Research Institute, 156 William Street, New York, New York 10038, USA*
[4]*Department of Biomedical Engineering, University of Southern California, Los Angeles, California 90089, USA*

(Received 8 November 2008; accepted 2 January 2009; published online 23 January 2009)

We report a photoacoustic imager that utilizes a focused laser beam in combination with a 20 MHz ultrasound focusing transducer to obtain micron-resolution tissue images over a long working distance. The imager is based on a ring transducer that combines ultrasonic and laser beams collinearly and confocally in a monolithic element. The combination of focused laser beam and short pulse irradiation led to significant improvement in lateral and axial resolutions compared to the pulse-echo ultrasonic imaging technique or photoacoustic imaging with an unfocused laser. Potential applications include clinical examination of the eye and characterization of thin and superficial tissues. © *2009 American Institute of Physics*. [DOI: 10.1063/1.3073749]

Ultrasound is an imaging method commonly performed in pulse-echo mode, where a focused acoustic pulse is emitted by the transducer into the tissue and echoes produced wherever the pulse encounters a discontinuity in acoustic impedance (density × speed of sound). Ultrasound biomicroscopy refers to frequencies of 30 MHz or more that have been used for high-resolution imaging of the eye[1,2] and skin.[3] Intraluminal probes in this frequency range are used for evaluation of vulnerable plaque.[4] Like all detection techniques based on waves, the resolution is of the order of one wavelength. For transducers with a center frequency of 20 MHz, the resolution is of the order of 200 μm. Although the resolution may be improved by using a higher frequency transducer, the exponential increase in absorption of ultrasound with increasing frequency sets the limit for useful operating frequency to about 50 MHz when a penetration depth greater than a few millimeters is needed.[5]

Recently, photoacoustic imaging, which combines optics and ultrasound to produce images, attracted considerable interest as a complementary diagnostic imaging technique.[4–8] The generation of photoacoustic signals is based on stress transients caused by thermal expansion of tissue in response to an absorbed light pulse. This rapid expansion of tissue generates a broadband acoustic pulse, which can then be detected by an ultrasound transducer. Cross-sectional images (B-scan) can be constructed from the time-resolved signals collected by an array of transducers or a single transducer with a scanning mechanism.[6] Images produced by the absorption-based contrast at a particular wavelength depicts an independent property from those imaged by pulse-echo ultrasound and may be used to highlight specific tissues of interest. For example, the laser wavelength may be tuned to the absorption peaks of oxy- or deoxyhemoglobin to highlight the structure of microvascular networks,[6] which cannot not be obtained with pulse-echo ultrasonic imaging.

Early photoacoustic imaging utilized light pulses to illuminate a large area and the spatial resolution was determined by the focal properties and frequency of the ultrasound transducer.[7,8] Recently, photoacoustic imagers that are capable of micron-level resolution have also been demonstrated. In this case, a focused laser is combined with the ultrasonic beam either at an angular offset between the axes of the two beams[9] or collinearly through a prism beam combiner.[10] The focused laser spot can be one to two orders of magnitude smaller than the focus of ultrasound resulting in a drastic improvement in resolution. High-resolution depiction of microvasculature has been reported.[10] The use of a beam combiner limited the working distance to a few millimeters[10] and the angled laser and ultrasonic axis had limited depth of field.[9]

In this paper we report the realization of high-resolution photoacoustic imaging based on a ring transducer, which allows focused laser and ultrasonic beams to be launched collinearly from a compact monolithic device toward a common focus. By eliminating the beam combiner, the working distance is extended by ten times to 3 cm. By focusing the laser to a spot far smaller than can be achieved with a transducer, lateral resolution can be significantly improved compared with that obtained with pulse-echo ultrasound or by photoacoustic imaging with a nonfocused light source. The coaxial arrangement of the laser and acoustic beams confers a superior depth of field compared to that produced in an angled arrangement. Potential applications of this imager include clinical diagnostic imaging of eye, including choroid and retina, which are less than 0.5 mm in thickness, but over 2 cm from the anterior surface of the globe, and microscopic imaging of superficial and thin tissues in general.

The experimental setup is shown in Fig. 1. The focusing ring transducer has a diameter of 1 cm with a 0.5 cm hole at the center to allow the laser beam to pass through. The focal length is 3 cm. The center frequency of the transducer is 20 MHz. A frequency-doubled passively Q-switched Cr, neodymium-doped yttrium aluminum garnet microchip laser

a)Electronic mail: y.c.chen@hunter.cuny.edu.

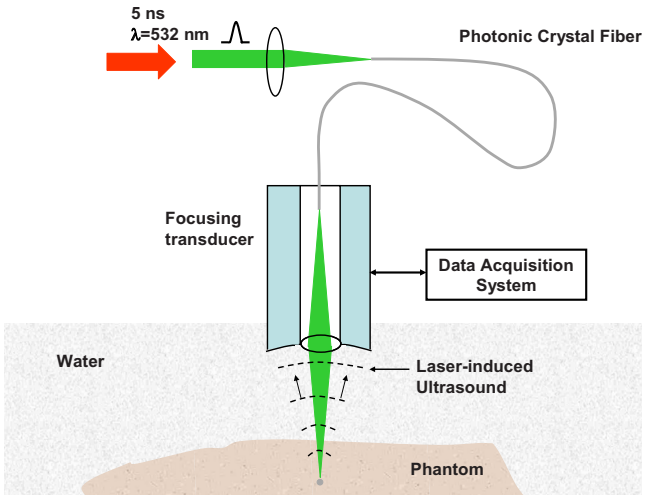

FIG. 1. (Color online) Schematic of the experimental setup.

emitting at 532 nm wavelengths is used as the irradiation source. The laser generates 5 ns pulses at a repetition rate of 500 Hz. The laser pulses are coupled into to a photonic crystal fiber with a core diameter of 20 μm. The fiber supports a single transverse mode with a Gaussian modal profile. The laser pulse energy is 1 μJ. A combination of time-resolved detection of the photoacoustic waves with a linear scanning along the lateral direction generates cross-sectional (B-scan) images. The system can also acquire pulse-echo ultrasound images for the same cross section for comparison. The samples included tissue-mimicking phantoms made of polyvinyl alcohol (PVA) with graphite particles on the surface or distributed within the volume and tissues including the ciliary body from a pig eye.

We first compare the lateral and axial resolutions of pulse-echo ultrasonic and photoacoustic imaging by examining the cross-sectional (B-scan) images of an aluminum wire in water at the same location. The images are shown in Fig. 2. The lateral full width at half maximum (6dB) width of the ultrasound image shown in Fig. 2(a) is measured to be 170 μm, which is consistent with the theoretical resolution of 180 μm based on the aperture and center frequency of the transducer. The lateral width measured with the photoacoustic imaging, shown in Fig. 2(b), is 35 μm, which is consistent with the wire diameter of 25 μm and the focused spot size of 20 μm. There is also a significant improvement in the axial resolution of the photoacoustic image compared to pulse-echo ultrasonic image. The photoacoustic signal caused by thermally induced stress transients are spikelike and shorter than the pulse-echo ultrasonic signal. The difference in signal bandwidth is illustrated in the typical oscilloscope traces and spectra shown in Fig. 2. From the 6dB bandwidths of the signals, the axial resolutions (=0.25 $\times$speed of sound/signal bandwidth) for pulse-echo ultrasonic and photoacoustic images are 46 and 20 μm, respectively.

Figure 3 shows the ultrasound and corresponding photoacoustic B-scan images of the same cross section in tissue-mimicking phantoms. The phantoms are made of 10% PVA in water with 25 μm sephadex particles suspended in the phantom to create ultrasonic and optical properties equivalent to those in soft tissues. The phantom has no absorption at 532 nm but strong optical scattering is present. The acoustic properties of PVA of the same composition are detailed in

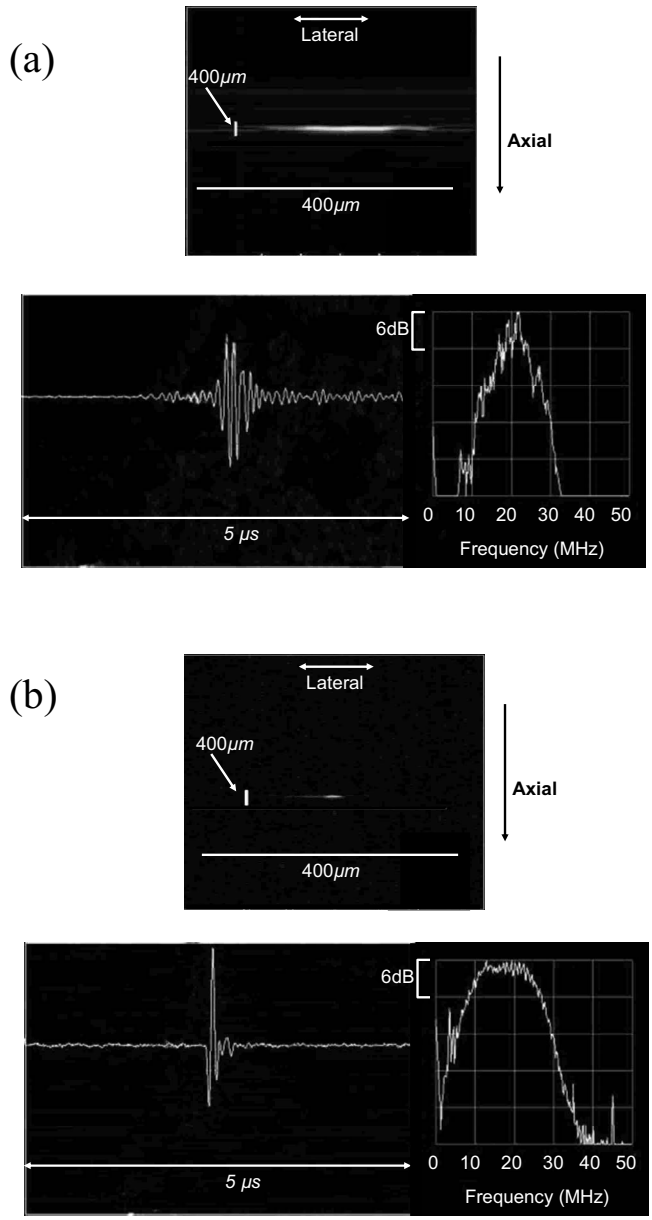

FIG. 2. (a) Pulse-echo ultrasonic and (b) photoacoustic images of an aluminum wire and corresponding oscilloscope traces and spectra of signals.

Ref. 11. We also created phantoms with 8 μm graphite particles, which strongly absorb light, either suspended in the phantom material volumetrically or only on the surface layer. The images in Fig. 3(a) are scans of graphite particles on the surface of the phantom. The surface features of the phantom are revealed with better clarity and higher resolution with the photoacoustic technique. Both imaging techniques reveal the presence of low-density graphite particles, which diffused into the phantom. The ultrasonic signals penetrate deeper into the sample while the photoacoustic signals have limited penetration depth, in this case, approximately 1 mm, once a strong absorbing structure along the line of sight is encountered. The images in Fig. 3(b) are scans of a phantom with graphite particles uniformly suspected throughout the volume. The photoacoustic image shows better clarity and higher resolution of randomly distributed particles. While some signals in the photoacoustic images and their corresponding ultrasonic signals are recognizable, the images of optical absorption and discontinuity of acoustic impedance are distinctly different in appearance. The images in Fig. 3(c)

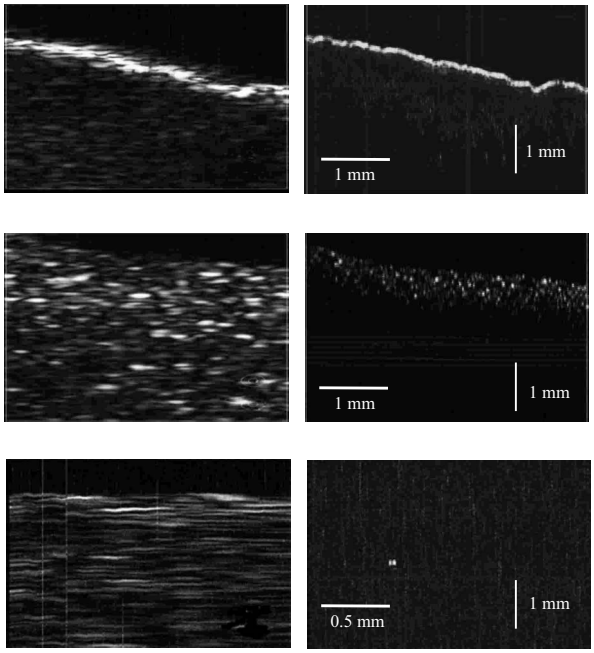

FIG. 3. Ultrasonic and pulse-echo photoacoustic images of the phantoms with (a) graphite powder on surface, (b) graphite powder uniformly suspended in volume, and (c) 75-μm-diameter hair embedded in phantom with 2% 25 μm sephadex scatterers.

are the cross-sectional views of a 75 μm hair at 1 mm below the surface of a phantom with 2% 15 μm diameter sephadex scatterers suspended throughout the volume. The hair is clearly resolved in the photoacoustic image but not in the ultrasonic image presumably due to the small discontinuity in the acoustic impedance of the hair in the phantom and the presence of acoustic scattering from the phantom material itself.

In optically scattering media such as biological tissues, the focused laser beam will expand due to lateral diffusion as it propagates deeper into the tissues. The advantage of high resolution is expected to hold within the transport mean free path, which, in soft tissues, is about 1 mm.[12] An example of high resolution imaging is given in Fig. 4, where the B-scan pulse-echo and photoacoustic images of the ciliary body of a pig eye are presented. The scan is done in a plane perpendicular to the ciliary processes. The ciliary body contains melanin, which strongly absorbs light, especially in the visible. 20 MHz pulse-echo ultrasound does not have sufficient resolution to resolve the processes, while the photoacoustic image, despite the scattering in the tissue, reveals individual processes with high resolution and clarity over at least a 2 mm depth.

The current study points to potential applications in clinical examination of superficial and thin tissues containing optically absorbing pigments such as melanin or hemoglobin, including skin, mucosa, and ocular tissues (iris, retina, and choroid). The design of the device is particularly suited for imaging of the retina and choroid, which are optically accessible through the transparent intervening ocular media (cornea, aqueous, pupil, lens, and vitreous). Because of the

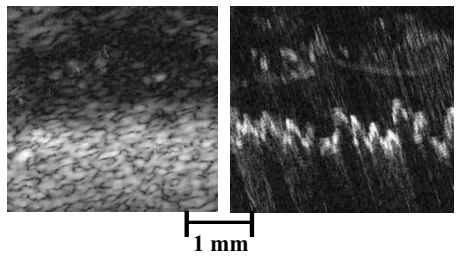

FIG. 4. (a) Pulse-echo and (b) photoacoustic images of the ciliary body of an excised pig eye. The B-scans were made in the plane perpendicular to the ciliary processes. The photoacoustic images reveal individual processes with high resolution and clarity not obtainable with the pulse-echo 20 MHz ultrasound.

24 mm axial length of a typical eye, ultrasound frequencies above about 20 MHz are impractical (due to absorption), limiting resolution on pulse-echo ultrasonography. The use of a focused laser will allow a near order-of-magnitude improvement in resolution over conventional ultrasound imaging of the retina/choroid.

In conclusion, we demonstrated the realization of high-resolution photoacoustic imaging, which allows microscopy examination of tissues over a long working distance. The system is based on a ring transducer, which allows focused laser and ultrasound beams to be launched from a compact monolithic device. The combination of focused laser beam and short pulse irradiation led to significant improvement in resolution in both the lateral and axial directions compared to the pulse-echo imaging technique. Potential clinical applications are discussed.

This work was supported by NIH Grant No. P41-EB002182, Grant No. UL1 RR024996 of the Clinical and Translational Science Center at Weill Cornell Medical College, the Dyson Foundation, the Biomedical Engineering Research Fund of the Riverside Research Institute, and Grant No. RR03037 from the National Center for Research Resources, a component of the National Institutes of Health.

[1]C. J. Pavlin, K. Harasiewicz, M. D. Sherar, and F. S. Foster, Ophthalmology **98**, 287 (1991).
[2]F. L. Lizzi, A. Kalisz, M. Aster, D. J. Coleman, R. H. Silverman, and D. Z. Reinstein, Acoust. Imaging **23**, 107 (1997).
[3]S. El-Gammal, K. Hoffman, and T. Auer, in *Ultrasound in Dermatology*, 1st ed., edited by K. Hoffman (Spinger, Germany, 1992), pp. 297–321.
[4]R. O. Esenaliev, A. A. Karabutov, and A. A. Oraevsky, IEEE J. Sel. Top. Quantum Electron. **5**, 981 (1999).
[5]C. G. A. Hoelen, F. F. M. de Mul, R. Pongers, and A. Dekker, Opt. Lett. **23**, 648 (1998).
[6]L. V. Wang, H. F. Zhang, and K. Maslov, *Biomedical Optics, Technical Digest (CD)* (Optical Society of America, 2006), Paper No. WD1.
[7]R. A. Kruger, W. L. Kiser, D. R. Reineche, and G. A. Kruger, Med. Phys. **30**, 856 (2003).
[8]S. Manohar, R. G. H. Willemink, F. van der Heijden, C. H. Slump, and T. G. vanLeeuwen, Appl. Phys. Lett. **91**, 131911 (2007).
[9]H. R. Silverman, H. O. Lloyd, T. Raevski, M. J. Rondeau, Y.-C. Chen, F. Kong, and D. J. Coleman, Proceedings of the 33rd International Symposium on Ultrasonic Imaging and Tissue Characterization, Arlington, VA, 14–16 May 2008 (unpublished), Paper No. 11.3.
[10]K. Maslov, H. F. Zhang, S. Hu, and L. V. Wang, Opt. Lett. **33**, 929 (2008).
[11]R. G. Holt and R. A. Roy, Ultrasound Med. Biol. **27**, 1399 (2001).
[12]H. F. Zhang, K. Maslov, G. Stoica, and L. V. Wang, Nat. Biotechnol. **24**, 848 (2006).